Nanoscale

Accepted Manuscript

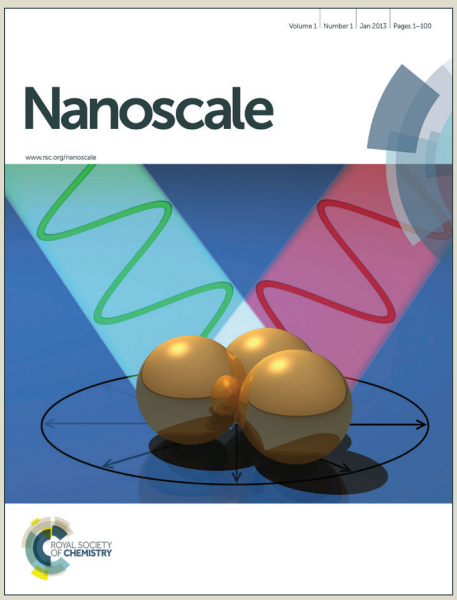

ROYAL SOCIETY OF CHEMISTRY

www.rsc.org/nanoscale

Structural and electronic properties of an ordered grain boundary formed by separated (1,0) dislocations in graphene

Chuanxu Ma, Haifeng Sun, Hongjian Du, Jufeng Wang, Aidi Zhao[a)], Qunxiang Li, Bing Wang[b)], and J. G. Hou

Hefei National Laboratory for Physical Sciences at the Microscale and Synergetic Innovation Center of Quantum Information & Quantum Physics, University of Science and Technology of China, Hefei, Anhui 230026, People's Republic of China

E-mail: adzhao@ustc.edu.cn; bwang@ustc.edu.cn

We present the investigation on the structural and electronic properties of an ordered grain boundary (GB) formed by separated pentagon-heptagon pairs in single-layer graphene/SiO_2 using scanning tunneling microscopy/spectroscopy (STM/STS), joint with density functional theory (DFT) calculations. It is observed that the pentagon-heptagon pairs, *i.e.*, (1,0) dislocations, form a periodic quasi-one-dimensional chain. The (1,0) dislocations are separated by 8 transverse rows of carbon rings, with period of ~2.1 nm. The protruded feature of each dislocation shown in the STM images reflects its out-of-plane buckling structure, which is supported by the DFT simulations. The STS spectra recorded along the small-angle GB show obvious differential-conductance peaks, the positions of which qualitatively accord with the van Hove singularities from the DFT calculations.

1 Introduction

A (1,0) dislocation, *i.e.*, a pentagon-heptagon pair, an edge dislocation with Burgers vector being a primitive vector of the cell, represents an important type of intrinsic topological defects in graphene.[1-5] Many other types of topological defects can be derived from the (1,0) dislocation,[5, 6] therefore, it is of great importance to understand the (1,0) dislocation. Theoretical calculations predict that there exists strong strain fields around single (1,0) dislocations.[7-9] The presence of the (1,0) dislocations with the associated strain fields may lead to out-of-plane buckling height of a few angstroms in graphene.[5, 6] According to the Read-Shockley model[10], aligning the (1,0) dislocations along a straight line can result in a discrete set of ordered small-angle grain boundaries (GBs) with low formation energy in graphene.[5, 6, 11] Recent studies showed the in-plane C-C bond deformation around the (1,0) dislocation in graphene[12, 13] and gave hints that the dislocation has an out-of-plane buckling structure.[14, 15] Lattice defects and curvature, which change the nearest-neighbor hopping between sublattices in graphene, give rise to perturbations in the low-energy linear dispersion, and it is thus expected to affect the electronic properties of graphene.[16, 17] Many theoretical works have been done for understanding the defect structures and their electronic properties,[8, 18-20] in particular, the so-called relatively ordered line defects. Even though, there is only a few experimental works that have provided direct evidence to connect the defect structures with their local electronic properties.[21] Using scanning tunneling microscopy/spectroscopy (STM/STS), some ordered and disordered GBs have been characterized.[22-25] Yang *et al.* have reported a promising way to form periodic GBs on Cu(111) surface from thermal reconstruction of the aperiodic ones.[26] Very recently, we confirmed the existence of the van Hove singularities (VHSs)[5, 19] in two types of ordered GBs,

i.e., a large-angle GB and a translational GB.[21] We are only aware of structural characterization of the (1,0) dislocations by STM,[27] however, their electronic properties have not been experimentally identified.

In this paper, we investigate another type of ordered GB that consists of the (1,0) dislocations in a single-layer graphene on a 300 nm SiO_2/Si substrate, using STM/STS performed at a low temperature of 80 K. The electronic properties of the GB as well as the atomic structure of single (1,0) dislocations are characterized. The experimental results qualitatively accord with the DFT calculations, which suggest that the GB consisting of quite separated (1,0) dislocations may still exhibit VHS states in the small-angle GB. This result is an important extension of our previous results on continuous ordered GBs,[21] and can also help to experimentally understand this type of GBs formed by (1,0) dislocations with various separations.[39]

2 Experiment and calculation details

The graphene sample was prepared by the low-pressure chemical vapor deposition (CVD) technique[28] with a recipe of CH_4 (50 sccm), H_2 (5 sccm) and Ar (440 sccm) under a pressure of ~10 Torr in a quartz tube at 950 °C for 10 minutes on a 25 μm thick polycrystalline copper foil. The as-grown graphene layer was transferred onto a 300 nm SiO_2/Si substrate by the PMMA-assisted wet-etching of the copper support method.[29, 30] The details about the sample preparation were described elsewhere.[21] The experiments were conducted using a low-temperature scanning tunneling microscope (UNISOKU Co., Ltd.) under ultrahigh-vacuum (UHV) conditions at 80 K. All the images were taken in a constant-current scanning mode. The current-voltage (*I*-*V*) and the

differential conductance (*dI/dV*) spectra were measured by turning off the feedback loop-gain. The *dI/dV* spectra were obtained using a lock-in amplifier with a sinusoidal modulation (f = 1000 Hz, V_{mod} = 5–10 mV). The polarity of the applied voltage refers to the sample bias with respect to the tip. Our calculations were carried out using density functional theory (DFT) with the projector-augmented wave method[31] as implemented in the Vienna *ab initio* simulation package (VASP).[32] The generalized gradient approximation functional in the PBE form[33] was adopted to treat the exchange and correlation potential. In the DFT calculation, the computational models involved two parallel equally spaced GBs within a rectangular supercell in order to satisfy periodic boundary conditions. We used a relatively large supercell size of d_x = 63.66 Å and d_y = 21.17 Å. This structural model is based on our experimental observations that the (1,0) dislocations are separated by 8 transverse rows of carbon rings, and the generic bisectors of the dislocations are slanted by a half carbon ring with each other. In this model, a unit cell includes 524 C atoms (see below in Fig. 3). The vacuum layer between the slabs was 10 Å. This GB structural model gave a tilting angle of 6.6° between the grains at both sides. The cutoff energy was set to be 400 eV, all atomic positions were fully relaxed until the residual forces decreased within 0.02 eV $Å^{-1}$, and the total energy was converged to 10^{-5} eV. A $1 \times 6 \times 1$ Monkhorst-Pack k-points mesh was used to sample the Brillouin zone of the small-angle GB. The STM image was simulated using an isovalue image based on Tersoff and Hamann's formula and its extension to simulate STM images.[34]

3 Results and discussion

Fig. 1(a) shows an atomically resolved STM image of a GB, consisting of six defects with almost

identical protruded features along a straight line. The profile along the arrowed line in Fig. 1(a) shows that the protrusions of the GBs have an average height of about 3 Å and are nearly periodically separated with a distance of about 2.1 nm [Fig. 1(b)], forming a quasi-one-dimensional (quasi-1D) periodic structure with a GB length of ~13 nm. Fig. 1(c) and 1(d) give the high resolution empty-state and filled-state STM images, in comparison with the simulated images, correspondingly. According to their good accordance, the observed protrusions can thus be well assigned to the (1,0) dislocations. In the topographic images, the bright spots are mainly located around the pentagon, while the heptagon is relatively dim. This is consistent with previous calculations that the charge density is enhanced around the pentagon and depressed near the heptagon in the (1,0) dislocation.[35, 36]

Fig. 1(e) shows the magnified image of the marked region by the rectangle in Fig. 1(a). A Burgers circuit taken around the (1,0) dislocation shows one lattice distance short in the direction perpendicular to the GB, corresponding to a Burgers vector of $\vec{b}$ = (1,0). It confirms our assignment of the (1,0) dislocation. A tilting angle of 6.5° is obtained between the grains at both sides of the GB, showing its small-angle GB feature. According to the atomic structure of the observed small-angle GB, a structural model is proposed in Fig. 1(f). The (1,0) dislocations are separated by 8 transverse rows of carbon rings, and the axes of (1,0) dislocations are slanted by a half carbon ring (the dashed blue lines), in consistent with the Read-Shockley model.[10] Following the notation we previously used,[18, 21] this small-angle GB can also be denoted as (-4,10)|(-5,10) GB. According to Frank's equation,[37] the tilting angle $\theta = 2\arcsin(|\vec{b}|/2d)$, where $|\vec{b}|$ = 2.46 Å is the length of the Burgers vector of the (1,0) dislocation, and d is one of the possible distance between

the dislocations. From the STM images, we have d = 2.1 nm, then it gives a tilting angle of 6.6°, in good agreement with the experimental observation. Fig. 1(g) shows a three-dimensional (3D) image of the (1,0) dislocation, whose protruded feature is consistent with the calculated out-of-plane buckling structure, as showed in Fig. 1(h). This feature is also similar to the image obtained from the single (1,0) dislocation of graphene on Ir(111) surface,[27] which has been attributed to the buckling structure, but its electronic property was not given. Here, the GB length (~13 nm) is relatively short, consistent with the suggestion that a longer straight GB is energetically unfavorable.[38] The existence of strain in the GB may be an important factor to prevent it to be longer.

We further measured the electronic properties of the small-angle GB, as shown in Fig. 2. The use of the insulating SiO_2 substrate can minimize the effect from the strong charge transfer between the graphene sheet and the metal substrate,[21] and can help to show up the intrinsic electronic properties of the (1,0) dislocations in graphene. Fig. 2(a) and 2(b) show the topographic image and the *dI/dV* map (acquired at +0.6 V), respectively. The tunneling conductance along the GB is obviously higher than graphene sheet away from the GB, with a width of ~1 nm, quite similar to our previous observations in other types of ordered GBs.[21] Fig. 2(c) and 2(d) give the *I-V* curves and the corresponding *dI/dV* curves acquired at different sites along the GB. The *dI/dV* curves [Fig. 2(d)] show quite similar features, where three peaks located at –0.4 V，+0.25 V and +0.6 V can be obviously seen, quite different from the pristine graphene site away from the GB by 2 nm (curve 11). From the feature of curve 11, the Dirac point (E_D) locates almost at the Fermi energy (E_F), indicating a low doping level of the graphene sheet.

To understand the electronic properties of the small-angle GB, we calculated the band structure and local density of states (LDOS). Fig. 3 gives the optimized structural model that we used in the calculations. To reduce the possibly introduced interactions between the GBs, the GBs are separated by 13 carbon rings in the *x* direction, *i.e.*, GBs separated by about ~3.1 nm. It has been shown that the error due to elastic interactions between the neighboring GBs can be effectively reduced if the separation between neighboring GBs is up to about 2 nm.[5] Therefore, the GB separation of ~3.1 nm used in our calculations should be enough to reduce the possible GB interactions. In addition, according to the experimental observations (Fig.1), we include the 8 transverse rows of carbon rings and the slanted axes of (1,0) dislocations. The optimized structure gives the unit cell of 63.66 × 21.17 $Å^2$.

The calculated results are given in Fig. 4. The empty and filled GB bands near the E_F are marked by the red and orange circles, where the sizes of the circles indicate the relative contributions of the states. There are four VHS singularities at the high symmetric points, *i.e.*, both of the empty and filled states at Γ and X points. Fig. 4(b) shows the calculated LDOSs obtained by averaging the DOSs over the 10 atoms of the (1,0) dislocation and the 6 atoms of the hexagon ring near the heptagon ring [marked by a dashed blue circle in Fig. 4(c)], in comparison with the experimental results (lower panel). In the calculation of the LDOSs, we have considered the weightings of the GB states, for showing the VHS states more clearly. The positions of the four VHS peaks (denoted as Γ_e, Γ_f, X_e, and X_f) are marked in the calculated LDOSs. It turns out that the main features in the calculated LDOS can qualitatively resemble those in the experimental *dI/dV* spectra of the GB [Fig. 4(b)]. Therefore, the experimentally observed peaks in the small-angle GB can be assigned to the

VHS states. The peak from the filled-state VHS at the Γ point (VHS-Γ_f) is quite weak due to its smaller weighting, which may explain the missing peak in the experimental spectra. However, the peak positions of the calculated LDOSs have obvious shifts in comparison with the experimental results. The difference in peak positions may be due to the accuracy of DFT in describing the GBs in graphene, such difference was also observed in other type of GBs.[21] Moreover, our DFT calculations give qualitatively consistent results with the ones obtained from the calculations using the tight-binding method,[39] although obvious difference in the splitting values of these states between two calculation methods. The difference can be attributed to the different computational methods and computational models. It demands to further theoretical investigation on the accuracy of the different calculation methods in describing the VHS states of graphene.

As to the spatial distributions, it is experimentally observed that the VHS states overall spread over almost all of the sites along the GB [Fig. 2(b)], although the VHS peaks show a certain degree of site-dependent behaviors [Fig. 2(d)]. Fig. 4(c) shows a considerable delocalized feature along the GB for the distribution of the calculated VHS states. For instance, the VHS-X_e shows an asymmetric feature in the spatial distribution along the GB. The distribution of VHS-X_e at the sites near the heptagon ring [marked by the blue circle in Fig. 4(c)] is relatively weak. This feature is also observed in the *dI/dV* spectra [curves 2 and 9 in Fig. 2(d)], where the peak (at ~0.6 V) of VHS-X_e becomes less pronounced, in consistent with the calculated LDOS at the site near the heptagon ring [blue curve in the upper panel of Fig. 4(b)]. We attribute such asymmetric distributions to the intrinsic asymmetric structure of each (1,0) dislocation (Fig. 1). We checked several GBs with smaller separations of (1,0) dislocations. Our DFT calculations indicate that the peak positions of

these VHS states tend to shift to higher energies with decreasing separation of (1,0) dislocations. Our experimental and theoretical results strongly indicate that the GB states are still delocalized, mainly distributed along the GB, even though the GB consists of the (1,0) dislocations separated from each other by 2.1 nm. Very recently, the calculations using the tight-binding method show that the finite separated distance between dislocations allows for the hybridization of the localized states.[39] The observed delocalized GB states can thus be attributed to the similar mechanism because of the hybridization of the VHS states.

4 Conclusion

In summary, we present a comprehensive understanding of the intrinsic structural and electronic properties of a small-angle GB, *i.e.*, (-4,10)|(-5,10) GB, consisting of the (1,0) dislocations in graphene. The atomic structure of the out-of-plane buckling in the (1,0) dislocation is characterized. The experimentally observed peaks in *dI/dV* spectra can be well attributed to the VHS states of the small-angle GB, which shows a periodic quasi-1D structure. The GB states show a quite delocalized feature, which is attributed to the hybridization of the relatively localized VHS states at finite separated distance of about 2.1 nm between the dislocations. Such small-angle GB represents a typical GB consisting of the widely concerned (1,0) dislocations. We believe that the identification of the structural and electronic properties of the small-angle GB, as well as the (1,0) dislocation, is important for understanding the effects of other GBs consisting of (1,0) dislocations in graphene.

5 Acknowledgements

This work was supported by National Key Basic Research Program (No. 2011CB921400, No. 2014CB921101), by the Strategic Priority Research Program (B) of the CAS (No. XDB01020100), and the National Natural Science Foundation of China (grants 91321309, 91421313, 51132007, and 21121003).

References

1. I. A. Ovid'ko, *Rev. Adv. Mater. Sci.*, 2012, 30, 201-224.
2. T.-H. Liu, C.-W. Pao and C.-C. Chang, *Carbon*, 2012, 50, 3465-3472.
3. J. Zhang, J. Gao, L. Liu and J. Zhao, *J. App. Phys.*, 2012, 112, 053713.
4. R. Grantab, V. B. Shenoy and R. S. Ruoff, *Science*, 2010, 330, 946-948.
5. O. V. Yazyev and S. G. Louie, *Phys. Rev. B*, 2010, 81, 195420.
6. T.-H. Liu, G. Gajewski, C.-W. Pao and C.-C. Chang, *Carbon*, 2011, 49, 2306-2317.
7. Y. Wei, J. Wu, H. Yin, X. Shi, R. Yang and M. Dresselhaus, *Nat. Mater.*, 2012, 11, 759-763.
8. Y. Liu and B. I. Yakobson, *Nano Lett.*, 2010, 10, 2178-2183.
9. A. Cao and Y. Yuan, *Appl. Phys. Lett.*, 2012, 100, 211912.
10. W. T. Read and W. Shockley, *Phys. Rev.*, 1950, 78, 275-289.
11. Z.-L. Li, Z.-M. Li, H.-Y. Cao, J.-H. Yang, Q. Shu, Y.-Y. Zhang, H. J. Xiang and X. G. Gong, *Nanoscale*, 2014, 6, 4309-4315.
12. A. Hashimoto, K. Suenaga, A. Gloter, K. Urita and S. Iijima, *Nature*, 2004, 430, 870-873.
13. J. H. Warner, E. R. Margine, M. Mukai, A. W. Robertson, F. Giustino and A. I. Kirkland, *Science*, 2012, 337, 209-212.
14. O. Lehtinen, S. Kurasch, A. V. Krasheninnikov and U. Kaiser, *Nat. Commun.*, 2013, 4, 2098.
15. J. H. Warner, Y. Fan, A. W. Robertson, K. He, E. Yoon and G. D. Lee, *Nano Lett.*, 2013, 13, 4937-4944.
16. A. H. Castro Neto, F. Guinea, N. M. R. Peres, K. S. Novoselov and A. K. Geim, *Rev. Mod. Phys.*, 2009, 81, 109-162.

17. V. Atanasov and A. Saxena, *Phys. Rev. B*, 2010, 81, 205409.

18. O. V. Yazyev and S. G. Louie, *Nat. Mater.*, 2010, 9, 806-809.

19. S. S. Alexandre, A. D. Lúcio, A. H. Castro Neto and R. W. Nunes, *Nano Lett.*, 2012, 12, 5097-5102.

20. J. Zhang and J. Zhao, *Carbon*, 2013, 55, 151-159.

21. C. Ma, H. Sun, Y. Zhao, B. Li, Q. Li, A. Zhao, X. Wang, Y. Luo, J. Yang, B. Wang and J. G. Hou, *Phys. Rev. Lett.*, 2014, 112, 226802.

22. J. Lahiri, Y. Lin, P. Bozkurt, I. I. Oleynik and M. Batzill, *Nat. Nanotech.*, 2010, 5, 326-329.

23. J. C. Koepke, J. D. Wood, D. Estrada, Z.-Y. Ong, K. T. He, E. Pop and J. W. Lyding, *ACS Nano*, 2013, 7, 75–86.

24. L. Tapasztó, P. Nemes-Incze, G. Dobrik, K. J. Yoo, C. Hwang and L. P. Biró, *Appl. Phys. Lett.*, 2012, 100, 053114.

25. P. Nemes-Incze, P. Vancsó, Z. Osváth, G. I. Márk, X. Jin, Y.-S. Kim, C. Hwang, P. Lambin, C. Chapelier and L. PéterBiró, *Carbon*, 2013, 64, 178-186.

26. B. Yang, H. Xu, J. Lu and K. P. Loh, *J. Am. Chem. Soc.*, 2014, 136, 12041–12046.

27. J. Coraux, A. T. N'Diaye, C. Busse and T. Michely, *Nano Lett.*, 2008, 8, 565-570.

28. X. Li, W. Cai, J. An, S. Kim, J. Nah, D. Yang, R. Piner, A. Velamakanni, I. Jung, E. Tutuc, S. K. Banerjee, L. Colombo and R. S. Ruoff, *Science*, 2009, 324, 1312-1314.

29. X. Li, Y. Zhu, W. Cai, M. Borysiak, B. Han, D. Chen, R. Piner, L. Colombo and R. S. Ruoff, *Nano Lett.*, 2009, 9, 4359-4363.

30. A. Reina, X. Jia, J. Ho, D. Nezich, H. Son, V. Bulovic, M. S. Dresselhaus and J. Kong, *Nano Lett.*, 2009, 9, 30-35.

31. P. E. Blöchl, *Phys. Rev. B*, 1994, 50, 17953-17979.

32. G. Kresse and J. Hafner, *Phys. Rev. B*, 1993, 47, 558-561.

33. J. P. Perdew, K. Burke and M. Ernzerhof, *Phys. Rev. Lett.*, 1996, 77, 3865-3868.

34. J. Tersoff and D. R. Hamann, *Phys. Rev. B*, 1985, 31, 805-813.

35. R. Tamura and M. Tsukada, *Phys. Rev. B*, 1994, 49, 7697-7708.

36. A. Cortijo and M. A. H. Vomediano, *Nucl. Phys. B*, 2007, 763, 293-308.

37. J. P. Hirth and J. Lothe, *Theory of Dislocations*, Wiley, New York, 1982.

38. Z. Zhang, Y. Yang, F. Xu, L. Wang and B. I. Yakobson, *Adv. Funct. Mater.*, 2014, DOI: 10.1002/adfm.201403024, n/a-n/a.

39. F. Gargiulo and O. V. Yazyev, *Nano Lett.*, 2014, 14, 250-254.

Figure Captions

Fig. 1 (a) Topographic STM image (+1.0 V, 50 pA; size: 10.1 × 18.5 nm^2) of a linear GB, consisting of individual (1,0) dislocations. The image is obtained by stitching two images with different scanning areas to show the whole length of the GB. (b) The line profile along the GB [the dashed blue line in (a)], showing a period of about 2.1 nm. (c) and (d) High resolution empty-state and filled images of the (1,0) dislocation from experiments (upper panel, ±1.0 V and 50 pA) and from simulations (lower panel), respectively, size: 2.1 × 2.3 nm^2. The structural model of the (1,0) dislocation is superposed. (e) Magnified topographic STM image (3.6 × 5.1 nm^2) of the area marked by the reactagle in (a). A Burgers circuit is plotted around a (1,0) dislocation. (f) Optimized structural model of two neighbored (1,0) dislocations, where the (1,0) dislocations are marked by symbols ⊥. The notation of the GB is shown. (g) 3D image of the (1,0) dislocation (–1.0 V, 50 pA). (h) Side view of the optimized structural model of the (1,0) dislocation, showing an out-of-plane buckling height of 2.8 Å.

Fig. 2 (a) STM topographic image (–1 V, 50 pA; size: 3.6 × 5.1 nm^2), and (b), *dI/dV* map (+0.6 V, 50 pA), acquired within the same area. (c) and (d) The *I-V* curves and the *dI/dV* curves (+1.0 V, 50 pA), respectively, correspondingly acquired at the marked sites 1-11 in (a). The experimental data are shifted vertically for clarity in (c) and (d). The dashed lines in (d) are for eyes guide only.

Fig. 3 The optimized structural model of GBs consisting of (1,0) dislocations. The simulation supercell and its size are indicated.

Fig. 4 (a) Calculated band structure of the small-angle GB. The x direction is defined perpendicular to the GB, and the y direction is parallel to the GB. The open circles denote the contributions from the GB states (red: empty states, orange: filled states). The inset shows a sketch of the corresponding "Brillouin zone". (b) Calculated LDOSs (upper panel) of (1,0) dislocation including 10 atoms belonging to the pentagon-heptagon pair and the hexagon ring [the marked blue circle in (c)] close to the heptagon ring, respectively, in comparison with the experimentally obtained *dI/dV* curves (lower panel). The LDOSs are obtained by summing the partial DOSs of the atoms and then averaging over the atom numbers. The experimental and theoretical data are shifted vertically for clarity. (c) Spatial distribution of the four VHS states, *i.e.*, Γ_e, X_e, Γ_f, and X_f. The isosurface value is 0.003 e/Å^3.

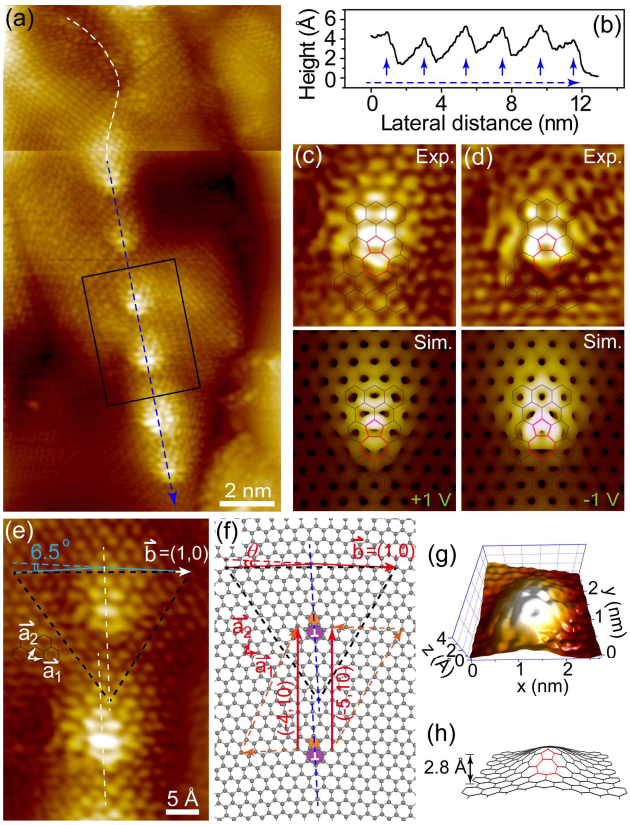

Fig. 1

Submitted to Nanoscale, by Ma *et al.*

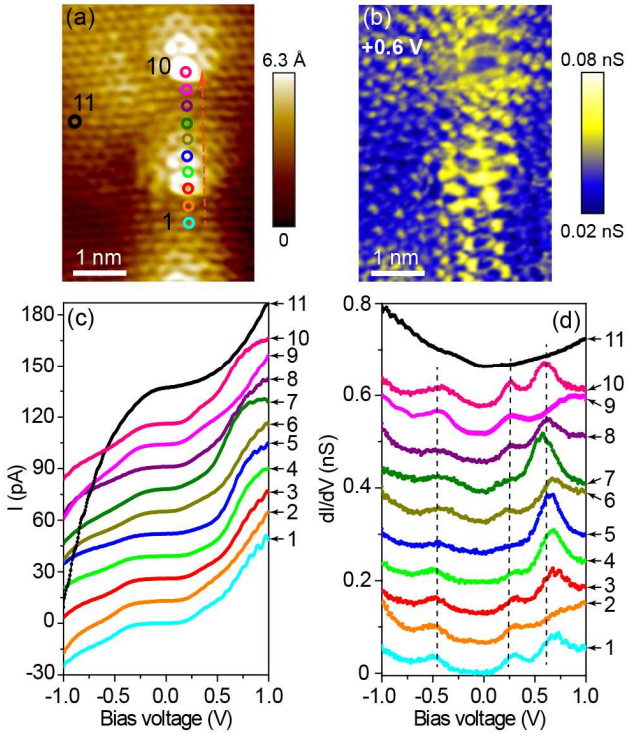

Fig. 2

Submitted to Nanoscale, by Ma *et al.*

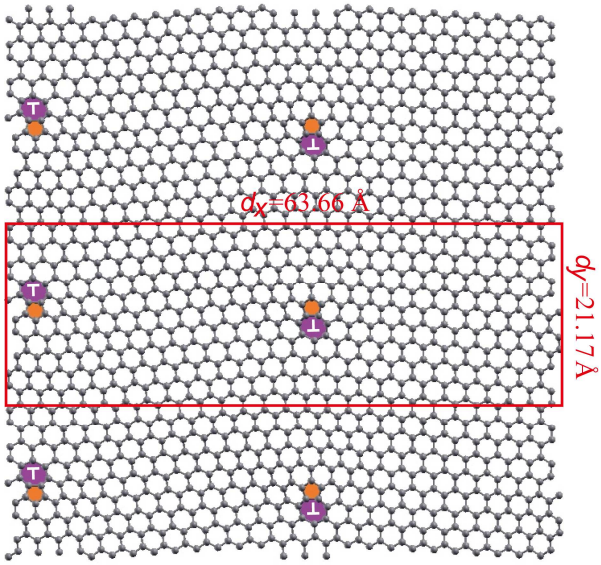

Fig. 3

Submitted to Nanoscale, by Ma *et al.*

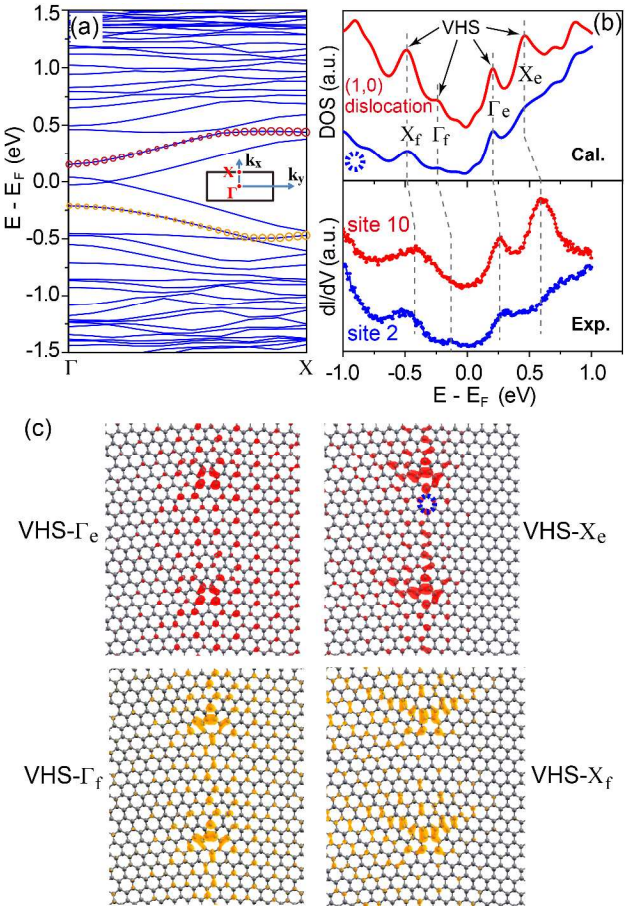

Fig. 4

Submitted to Nanoscale, by Ma *et al.*

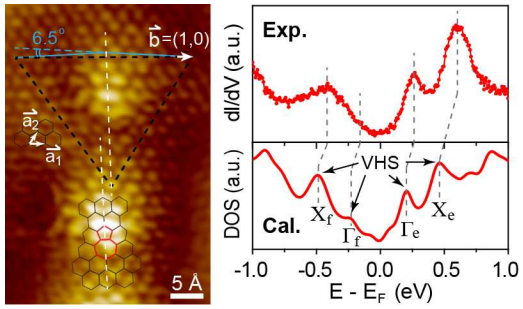

Graphical abstract